Available online at www.sciencedirect.com

ScienceDirect

journal homepage: www.elsevier.com/locate/ijrefrig

A study of working fluids for heat driven ejector refrigeration using lumped parameter models

Giorgio Besagni[*], *Riccardo Mereu*, *Giuseppe Di Leo*, *Fabio Inzoli*

Politecnico di Milano, Department of Energy, Via Lambruschini 4, 20156, Italy

ARTICLE INFO

Article history:
Received 22 November 2014
Received in revised form
25 May 2015
Accepted 18 June 2015
Available online 26 June 2015

Keywords:
Ejector
Working fluids
COP
Entrainment ratio
Ejector refrigeration
Ejector efficiencies

ABSTRACT

This paper studies the influence of working fluids over the performance of heat driven ejector refrigeration systems performance by using a lumped parameter model. The model used has been selected after a comparison of different models with a set of experimental data available in the literature. The effect of generator, evaporator and condenser temperature over the entrainment ratio and the COP has been investigated for different working fluids in the typical operating conditions of low grade energy sources. The results show a growth in performance (the entrainment ratio and the COP) with a rise in the generator and evaporator temperature and a decrease in the condenser temperature. The working fluids have a great impact on the ejector performance and each refrigerant has its own range of operating conditions. R134a is found to be suitable for low generator temperature (70–100 °C), whereas the hydrocarbons R600 is suitable for medium generator temperatures (100–130 °C) and R601 for high generator temperatures (130–180 °C).

Une étude à l'aide des modèles à paramètres localisés de fluides actifs pour un système frigorifique à éjecteur conduit par de la chaleur

Mots clés : Ejecteur ; Fluides actifs ; COP ; Taux d'entrainement ; Système frigorifique à éjecteur ; Efficacités d'éjecteur

* *Corresponding author*. Politecnico di Milano, Department of Energy Via Lambruschini 4a, 21056 Milan, Italy. Tel.: +39 02 2399 3826.
E-mail addresses: giorgio.besagni@polimi.it (G. Besagni), riccardo.mereu@polimi.it (R. Mereu), giuseppe3.dileo@mail.polimi.it (G. Di Leo), fabio.inzoli@polimi.it (F. Inzoli).

http://dx.doi.org/10.1016/j.ijrefrig.2015.06.015

Nomenclature

Symbols

A	area [m^2]
CE	computational effort [–]
COP	coefficient of performance [–]
D	diameter [m]
E_R	relative error [–]
GWP	global warming potential [–]
$\dot{L}_p$	pump power [W]
k	heat capacity ratio [–]
$\dot{m}$	mass flow rate [kg s^{-1}]
ODP	ozone depletion potential [–]
p	pressure [Pa]
$\dot{Q}$	rate of heat [W]
T	temperature [°C]
u	velocity [m s^{-1}]
X	general quantity

Greek symbols

η	isentropic efficiency [–]
ϕ	throat area ratio, $\phi = A_2/A_t$ [–]
φ, ψ	loss coefficient [–]
ω	entrainment ratio [–]

Superscripts

′	isentropic condition
*	critical mode operation of ejector

Subscripts

1	nozzle exit section
2	constant area section
c	condenser
d	diffuser
e	evaporator
exp	experimental data
g	generator
m	mixing chamber
mod	calculated value from the model
n	nozzle
p	primary fluid
s	secondary fluid
t	nozzle throat section
y	mixing section

1. Introduction

The global warming and the increasing need for the thermal comfort have led to a rapidly increasing cooling energy and electricity demand. Thermal energy refrigeration would allow a significant reduction of these problems and ejector refrigeration systems seem a promising alternative because of its structural simplicity, low capital cost, reliability, little maintenance, low initial and running cost and long lifespan (Vidal and Colle, 2010). An ejector (Fig. 1) is able to provide a combined effect of compression, mixing and entrainment with no-moving parts and without limitations concerning working fluids. For these reasons, ejector refrigeration systems can be used in buildings, in distributed tri-generation systems and for the waste heat recover from industrial processes (Ben Mansour et al., 2014; Godefroy et al., 2007; Little and Garimella, 2011). Nevertheless, the ejector refrigeration has not been able to penetrate the market because of the low coefficient of performance (Sarkar, 2012): this is because the efficiency of the whole system is highly influenced by ejector performances, which significantly depends on the geometry, working fluid and operating conditions (Kasperski and Gil, 2014; Selvaraju and Mani, 2006; Varga et al., 2009a; Yapıcı et al., 2008). This paper deals with the screening of the working fluids, using a validated lumped parameter model, in the range of operating conditions of low grade energy sources (waste heat and solar energy sources). If compared with the other papers concerning working fluid for ejector refrigeration systems (Chen et al., 2014b,c; Kasperski and Gil, 2014), the present one provides a coupled evaluation of working fluids and ejector models. This paper is divided in three parts. In the first part, the role of working fluids over ejector performance is outlined with a brief literature survey. In the second part, five different ejector models are evaluated and compared over a large set of experimental data concerning different operating conditions, working fluids and geometry. In the third part, on the basis of the above mentioned analysis, the model of Chen et al. (2014a) is selected and is used for studying the influence of working fluids over ejector performance and indications for ejector models and working fluids are provided in the conclusions.

2. Working fluids for ejector refrigeration

A suitable refrigerant for refrigeration system should yield good performance in the selected operating ranges. Generally speaking, the following requirements must be taken into account (Abdulateef et al., 2009): the thermo-physical properties (latent heat of vaporization, critical temperature, the viscosity, thermal conductivity, the molecular mass, ecc), the environmental impact (zero ozone depletion potential "ODP", low global warming potential "GWP") and the working fluid should be chemically stable, non-toxic, non-explosive, non-corrosive, cheap and available on the market (please notice that in the follow we refer to the ASHRAE Standard 34, taking into account recent updates of the designation and safety classification of refrigerants that introduce the new flammability class 2L (ASHRAE, 2010)). Furthermore, when selecting working fluids can be classified accordingly with the saturated vapor line slope in the T–s diagram (Chen et al., 2014c): wet or dry. When considering ejector refrigeration systems, a large number of refrigerants have been used.

In early 1900s, the first working fluid employed in a jet refrigerator was water: it has a high heat of vaporization, is inexpensive and has minimal environmental impact.

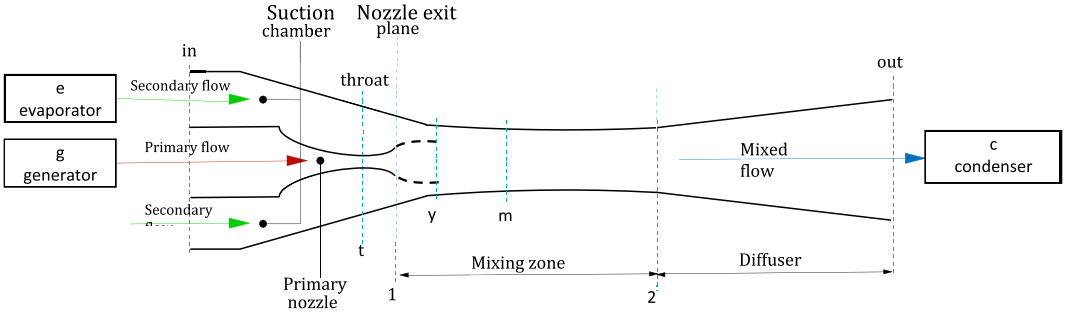

Fig. 1 – Ejector layout.

However, there are some drawbacks when using water as a working fluids: the cooling temperature is limited above to 0 °C, the system must be under vacuum condition and obtainable *COP* is not high (less than 0.5) (Angelino and Invernizzi, 2008). Since halocarbon refrigerants emerged from 1930s, they have been extensively studied in ejector refrigeration systems. These systems can provide cooling temperature below 0 °C and can exploit low-grade thermal energy (i.e. as low as 60 °C), producing an acceptable *COP* (0.4–0.6) (Chen et al., 2013b).

In 1987, the Montreal Protocol was ratified and among the banned products, there were several halocarbon compounds widely used in refrigeration applications (i.e., chlorofluorocarbon (CFCs) and hydrochlorofluorocarbon (HCFCs)), thus forcing researchers to turn to natural refrigerants and hydrocarbons. The HFCs do not deplete the ozone layer and have many of the desirable properties of CFCs and HCFCs (del Valle et al., 2014). They have significant benefits regarding safety, stability and low toxicity, being appropriate for large-scale applications (Sarbu, 2014). Even more promising for the future are the HFOs. They can offer balance among performance (*COP* = 0.2–0.35), environmental impact, safety and durability. However, they belong to A2L safety group and thus they will require changes to equipment safety standards. In additions to the new halocarbon compounds, also the HCs with low environment impact are considered as promising alternatives (Kasperski and Gil, 2014). Unfortunately, the HC refrigerants are highly flammable, which limits the usage in large capacity systems. These concerns can be relieved designing safer plant or with additional research about new mixture between HCs and HFCs.

New halocarbon compounds and HCs are ozone-friendly, but they have significant GWP, therefore, possible alternatives have been proposed, such as: ammonia, methanol and carbon dioxide. Ammonia NH_3 (R717) has been proposed as refrigerant for its advantages (Sankarlal and Mani, 2007): low cost, high performance (and thus low energy cost), more favorable thermodynamic properties and it is environmental friendly. Some applications, for NH_3, are reported in the industrial field and small absorption refrigerators for domestic use, however, some concerns exist considering its toxicity, that may limit its use (Bolaji and Huan, 2013; Chen et al., 2013b). Another interesting option is the Methanol, which can be a valid solution in refrigeration systems because of to its thermo-physical properties, low environmental impact and low cost; however, it is toxic and highly flammable (Alexis and Katsanis, 2004). Carbon dioxide is also considered as a promising working fluid, because is a non-flammable natural substance with zero ODP and a lower GWP compared to other substances (Lucas and Koehler, 2012).

In the recent years, the regulations are becoming stricter in terms of the environment protection. The EU Regulation 517/2014 is going to phase out and limit the use of refrigerants with high GWP value, like R134a, R404a and R410a. Therefore, environmentally friendly halocarbons, hydrocarbons, natural refrigerants (R717, R744) and HFC/HFO mixtures will be increasingly employed (Mota-Babiloni et al., 2015).

3. Lumped parameter models

3.1. *Models employed*

In lumped parameter models, the mass, momentum and energy conservation equations are used to evaluate ejector performances. All these equations are coupled and some assumptions are postulated in order to simplify the problem, such as (i) steady state and (ii) one dimensional flow and (iii) adiabatic system. In this study five mathematical models from the literature to predict ejector performance have been considered (Cardemil and Colle, 2012; J. Chen et al., 2014a; W. Chen et al., 2013a; Kumar and Ooi, 2014; Zhu et al., 2007). These models, with different mathematical formulations, have been selected among the most recent models proposed in the literature. The performance of these models has not been evaluated yet. Moreover, the models considered in this study can be seen as an advancement of the previous models that have been widely used in the literature also as reference and comparison for the recent ones. A literature review on the previous lumped parameter models and their performance can be found in the review of He et al. (2009). In Table 1 are summarized the models main assumptions, the required input parameters, the output results and the code used for each model under studying. The original papers report the calculation procedure and the simplifying assumptions necessary to the resolution of the problem. The present work has followed their solution methods.

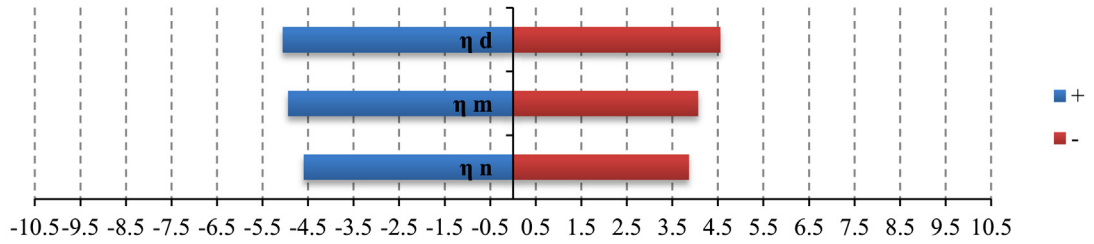

a) Model 1 – η_n: -4.59-3.87%; η_m: -4.94-4.07%; η_d: -5.06-4.56%.

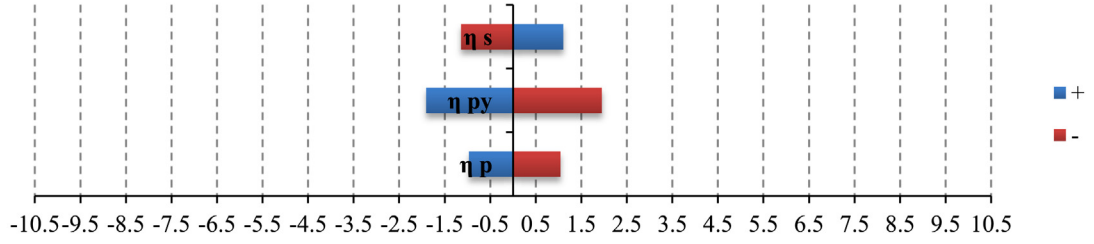

b) Model 2 – η_p: -0.96-1.04%; η_{py}: -1.91-1.95%; η_s: -1.14-1.10%.

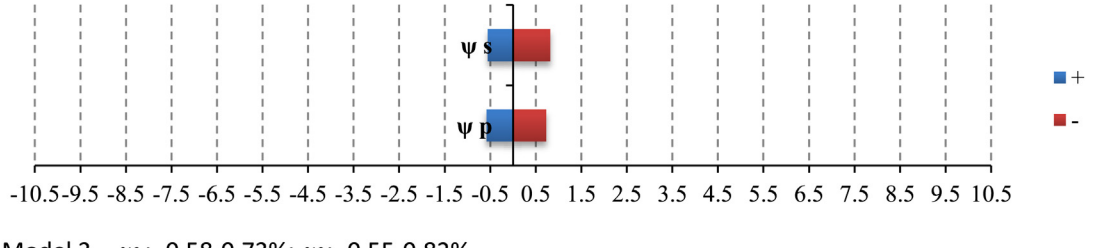

c) Model 3 – ψ_p: -0.58-0.73%; ψ_s: -0.55-0.82%.

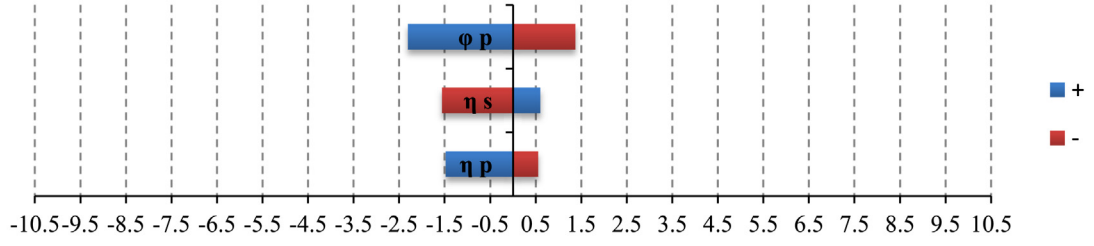

d) Model 4 – η_p: -1.48-0.56%; $\eta_{s:}$: -1.56-0.60%; φ_p: -2.31-1.37%.

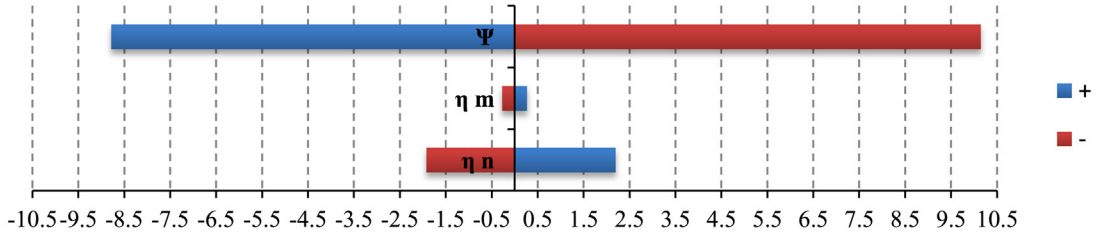

e) Model 5 – η_n: -1.92-2.20%; η_m: -0.27-0.26%; ψ: -8.78-10.15%.

Fig. 2 – Ejector component efficiencies sensitivity analysis.

The balance equations of these models have been implemented in the MATLAB® R2013a framework and the thermodynamic properties of the working fluids have been evaluated by using the thermophysical property library CoolProp (v 4.1.2) (Bell et al., 2014). In the original papers are instead used the NIST database (M1, M2, M3 and M4) or the EES software (M5).

Table 1 – Lumped parameter models: main hypotheses and boundary conditions.

Code	Model	Main hypotheses	Input parameters	Output parameters	Mixing efficiency and loss definition
M1	(Chen et al., 2014a)	Isentropic expansion of the secondary flow from inlet to nozzle exit; Ideal gas with k = cost.	T_g, T_e, p_c k η_n, η_m, η_d	ω, ϕ, COP	$\eta_m = \frac{u_2^2}{u_{2'}^2}$
M2	(Chen et al., 2013a)	Primary flow does not mixing with the secondary flow up to at y–y section; Ideal gas with k = cost and C_p = cost.	T_g, p_g, T_e, p_e, p_c A_t, A_1, A_2 k, C_p η_p, η_{py}, η_s, ψ_m	ω	$\psi_m = \frac{(m_p+m_s)u_m}{m_p u_{py}+m_s u_{sy}}$
M3	(Zhu et al., 2007)	Parameters uniformly distributed in the radius r direction; Secondary flow reaches chocking condition at cross section y–y; Ideal gas with k = cost.	T_g, p_g, T_e, p_e, p_c A_t, A_1, A_2 k ψ_p, ψ_s	ω, COP	–
M4	(Kumar and Ooi, 2014)	Secondary flow reaches chocking condition at cross section y–y; Normal shock fixed at the end of the mixing chamber; Ideal gas with $k = f(T)$.	T_g, p_g, T_e, p_e A_t, A_1, A_2 η_p, φ_p, η_s, η_d	ω, T_c	–
M5	(Cardemil and Colle, 2012)	Primary flow does not mixing with the secondary flow up to at y–y section; Mixing process start after the chocking of the secondary flow; Real gas effect.	T_g, p_g, T_e, p_e, p_c A_t, A_1, A_2 η_n, η_m, η_d, φ_m	ω, COP	$\eta_m = \frac{h_{p1}-h_{py}}{h_{p1}-h_{py'}}$ $\varphi_m = \frac{(m_p+m_s)u_m}{m_p u_{py}+m_s u_{sy}}$

The benchmarks used for evaluating the performance of these models are experimental data taken from the literature:

[i] Huang examined 11 different ejectors (ϕ = 6.44–10.64) using R141b as working fluid, obtaining 39 sets of data under various operating conditions (T_g = 78–95 °C, T_e = 8–12 °C and T_c = 28–36 °C). The various configurations were obtained using 2 nozzles (A_1/A_t = 2.905–3.271) and 8 different mixing chambers (D_2 = 6.7–9.2 mm) (Huang et al., 1999);

[ii] Ablwaifa ran his experiment at different operating conditions using R236fa (ϕ = 7.44, T_g = 82–88 °C, T_e = 4–12 °C and T_c = 27–33 °C) and R245fa (ϕ = 11.46, T_g = 100–120 °C, T_e = 8–15 °C and T_c = 34–46 °C) as working fluid (Ablwaifa, 2006), obtaining 9 and 20 sets of data, respectively.

Our results have been also compared with the original model results. Huang have been widely used for validating the model performance in the original references and we have also used this benchmark in order to evaluate the influence of the model implementation on the results (i.e. tolerances, thermodynamic library, etc). The effectiveness of the models is evaluated in terms of the relative error E_R defines as:

$$E_R(X) = \left|\frac{X_{mod} - X_{exp}}{X_{exp}}\right| 100 \quad (1)$$

where X_{exp} and X_{mod} are the measurement and the model estimates, respectively.

In the last part of the paper the influence of the working fluids over ejector and system performance has been evaluated. For refrigeration application, the most important parameters employed to describe ejectors performance are the entrainment ratio ω and the coefficient of performance COP of the thermodynamic cycle. The entrainment ratio ω is given by the ratio between mass of secondary flow $\dot{m}_e$ and mass of primary flow $\dot{m}_g$

$$\omega = \frac{\dot{m}_e}{\dot{m}_g} \quad (2)$$

The coefficient of performance COP is defined as the ratio between evaporation heat energy $\dot{Q}_e$ (cooling effect) and the total incoming energy in the cycle $\dot{Q}_g + \dot{L}_p$.

$$COP = \frac{\dot{Q}_e}{\dot{Q}_g + \dot{L}_p} \quad (3)$$

3.2. *Models evaluation*

The goal of this section is mainly to define an appropriate model for evaluating the working fluid influence over the ejector performance, dealt in the second part of the paper. For this purpose, a general and accurate model should be selected. Indeed, both these characteristics are fundamental to carry out a reliable analysis:

- the evaluation of the wide-ranging characteristic of the model is based on the mathematical structure of the model and its dependency on the ejector geometry and operating conditions;
- the evaluation of the accuracy of the models based, instead, on the correct prediction of entrainment ratio, measured by the relative errors (Eq. (1)).

For each analyzed model, the results published in the original paper are compared to the ones obtained in the current study. The assumption made about ejector efficiencies

Table 2 – Models comparison.

Model	Benchmark	Fluid	Efficiencies [–]	E_R [%] min, max, mean, variance
M1	Yapıcı et al., 2008	R123	$\eta_n = 0.9$, $\eta_m = 0.85$, $\eta_d = 0.9$	E_R (ϕ): n.a., 6.5, n.a., n.a. E_R (ω): n.a.
	Huang et al., 1999	R141b	$\eta_n = 0.95$, η_m = G.D., η_d = G.D.	E_R (ϕ): 0.12, 5.87, 1.67, 2.14 E_R (ω): 0.07, 29.03, 11.84, 80.97
Current study	Huang et al., 1999	R141b	$\eta_n = 0.95$, η_m = G.D., η_d = G.D.	E_R (ϕ): 0.05, 5.54, 1.75, 2.25 E_R (ω): 1.25, 38.98, 17.53, 129.97
	Ablwaifa, 2006	R236fa	$\eta_n = 0.95$, $\eta_m = 0.9$, $\eta_d = 0.85$	E_R (ϕ): 2.59, 6.83, 4.9, 1.73 E_R (ω): 0.4, 28.67, 12.01, 110.26
	Ablwaifa, 2006	R245fa	$\eta_n = 0.95$, $\eta_m = 0.9$, $\eta_d = 0.85$	E_R (ϕ): 0.02, 1.81, 0.55, 0.28 E_R (ω): 0.36, 47.76, 17.39, 279.85
M2	Huang et al., 1999	R141b	$\eta_p = 0.95$, $\eta_{py} = 0.88$, $\eta_s = 0.85$, ψ_m = G.D.	E_R (ω): 0.06, 14.2, 4.56, 12.66
	Hemidi et al., 2009	Air	$\eta_p = 0.95$, $\eta_{py} = 0.88$, $\eta_s = 0.85$, $\psi_m = 0.84$	E_R (ω): n.a., 19.8, n.a., n.a.
	(Chen et al., 2013a)	R290	$\eta_p = 0.98$, $\eta_{py} = 0.95$, $\eta_s = 0.85$, $\psi_m = 0.84$	E_R (ω): n.a., 20, n.a., n.a.
Current study	Huang et al., 1999	R141b	$\eta_p = 0.95$, $\eta_{py} = 0.88$, $\eta_s = 0.85$, ψ_m = G.D.	E_R (ω): 0.04, 23.9, 6.11, 28.88
	Ablwaifa, 2006	R236fa	$\eta_p = 0.95$, $\eta_{py} = 0.88$, $\eta_s = 0.85$, $\psi_m = 0.82$	E_R (ω): 0.03, 8.42, 3.37, 5.37
	Ablwaifa, 2006	R245fa	$\eta_p = 0.95$, $\eta_{py} = 0.88$, $\eta_s = 0.85$, $\psi_m = 0.8$	E_R (ω): 1.47, 16.81, 10.31, 14.44
M3	Huang et al., 1999	R141b	$\psi_p = 0.95$, $\psi_s = 0.85$	E_R (ω): 0.18, 10.78, 4.52, 9.65
	Aphornratana et al., 2001	R11	$\psi_p = 0.9$, $\psi_s = 0.85$	E_R (ω): n.a., 12.39, n.a., n.a.
Current study	Huang et al., 1999	R141b	$\psi_p = 0.95$, $\psi_s = 0.85$	E_R (ω): 0.01, 10.7, 4.61, 9.62
	Ablwaifa, 2006	R236fa	$\psi_p = 0.95$, $\psi_s = 0.85$	E_R (ω): 0.12, 16.08, 5.4, 40.98
	Ablwaifa, 2006	R245fa	$\psi_p = 0.95$, $\psi_s = 0.85$	E_R (ω): 9.59, 22.31, 17, 11.33
M4	Huang et al., 1999	R141b	$\eta_p = 0.95$, $\varphi_p = 0.88$, $\eta_s = 0.85$, $\eta_d = 0.9$	E_R (ω): n.a., n.a., 4, n.a. E_R (T_c): n.a., 11, 5, n.a.
Current study	Huang et al., 1999	R141b	$\eta_p = 0.95$, $\varphi_p = 0.88$, $\eta_s = 0.85$, $\eta_d = 0.9$	E_R (ω): 0.09, 27.49, 6.95, 39.7 E_R (T_c): 7.39, 12.58, 10.18, 1.92
	Ablwaifa, 2006	R236fa	$\eta_p = 0.95$, $\varphi_p = 0.88$, $\eta_s = 0.85$, $\eta_d = 0.9$	E_R (ω): 2.96, 15.23, 8.64, 15.43 E_R (T_c): 5.35, 6.89, 6.23, 0.25
	Ablwaifa, 2006	R245fa	$\eta_p = 0.95$, $\varphi_p = 0.88$, $\eta_s = 0.85$, $\eta_d = 0.9$	E_R (ω): 1.91, 18.65, 10.67, 16.73 E_R (T_c): 10.42, 17.84, 13.83, 3.83
M5	Huang et al., 1999	R141b	$\eta_n = 0.95$, $\eta_m = 0.85$, $\eta_d = 0.95$, φ_m = G.D.	E_R (ω): 0.21, 8.88, 3.06, 4.87
Current study	Huang et al., 1999	R141b	$\eta_n = 0.95$, $\eta_m = 0.95$, $\eta_d = 0.95$, φ_m = G.D.	E_R (ω): 0.32, 8.85, 3.17, 4.94
	Ablwaifa, 2006	R236fa	$\eta_n = 0.95$, $\eta_m = 0.95$, $\eta_d = 0.95$, $\varphi_m = 0.92$	E_R (ω): 0.52, 10.64, 6.87, 14.57
	Ablwaifa, 2006	R245fa	$\eta_n = 0.95$, $\eta_m = 0.88$, $\eta_d = 0.85$, $\varphi_m = 0.9$	E_R (ω): 7.78, 17.78, 13.66, 8.21

G.D. means geometry dependent accordingly with the formulation in the original reference of the model.

and the performances achieved by the models are summarized in Table 2. The ejector efficiency values reported are the same used by the authors of the models M1, M2, M3, M4 and M5 when investigating the benchmark provided by Huang et al. For the benchmarks provided by Ablwaifa, the efficiency parameters that depend on geometry were calculated with the correlations reported in the original reference of the models. The definitions of all the ejector efficiencies used are in accordance with the original references and, although the ejector efficiencies depend on the specific working fluid, working conditions and geometrical configurations (Varga et al., 2009b), they are assumed as constant in agreement with the considered lumped parameter models and the literature of analytical studies (Huang et al., 1999; Kasperski and Gil, 2014). However, as the mixing loss coefficient was found to vary slightly with the ejector geometry, many works in literature calculated it using a convenient relation as a function of the ejector area ratio. The ejector efficiencies used are isentropic for primary nozzle, the suction chamber and the diffuser. The formulations of the mixing efficiencies are reported in Table 1. Some models, i.e. M1, M2 and M5, calculate the mixing efficiency and loss coefficient from energy balance considerations; the other ones, i.e. M3 and M4, instead, implement them making use of some assumptions or correlations. In any case, they express the friction and mixing losses, due to the interaction between the primary and secondary flows, occurring throughout the mixing chamber. These losses can be a significant source of irreversibility and, therefore, affect the ejector performance. A comparison of the formulation of these efficiencies have been performed by Varga et al. (2009b) and by Banasiak et al. (2014). In this study, a sensitivity analysis over the ejector efficiency values is presented in Section 3.2.2 and it shows that the loss coefficients have a great influence on the results if compared with the other efficiencies.

Figs. 3–8 represent the results for the M1, M2, M3, M4 and M5 model: each figure consists of three graphs (one for each benchmark) that provide the parity plot between the results of this study and the experimental data, with histograms of the relative errors distribution. Fig. 3 represents the prediction of the geometric parameter ϕ (=A_2/A_t) for the model M1, Figs. 4–8 represent the prediction of the entrainment ratio for the M1, M2, M3, M4 and M5 model, respectably. In particular, the histogram allows comparing directly the results achieved for the different working fluids. In the last part of this section, a sensitivity analysis for studying the influence of the ejector component efficiencies has been performed.

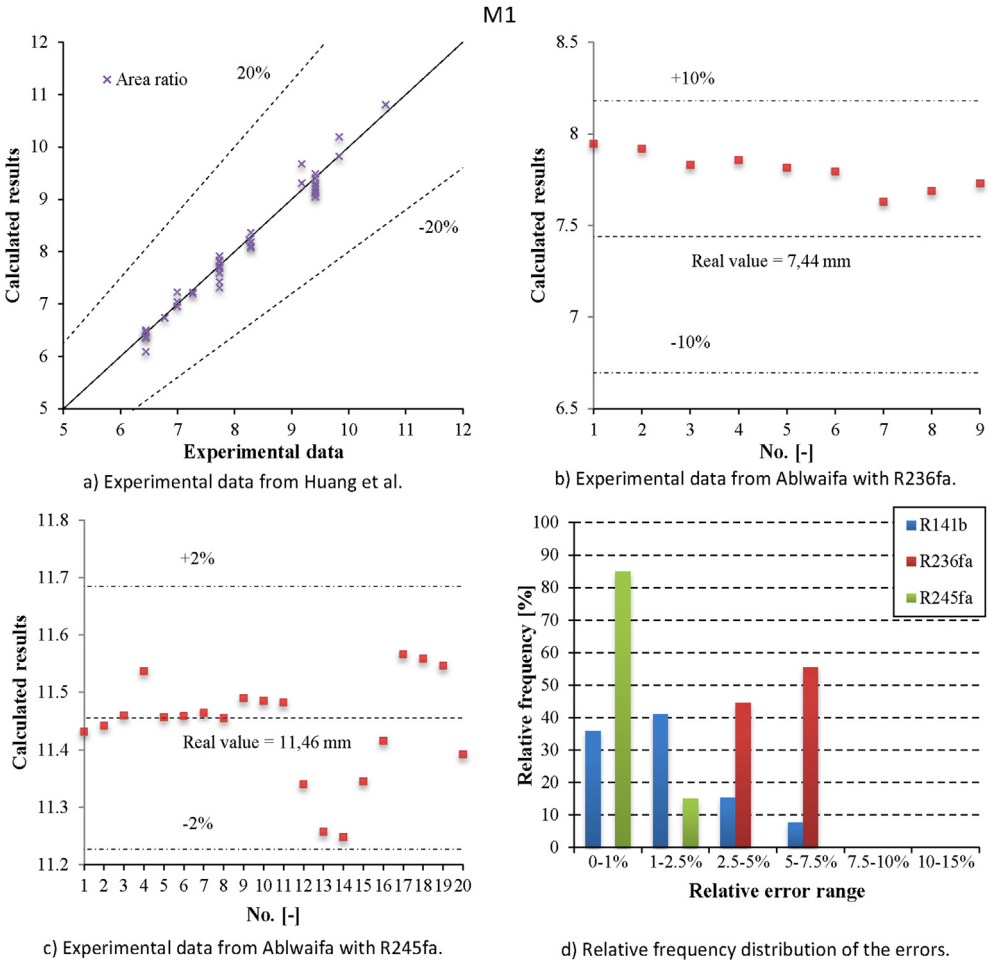

Fig. 3 – Comparison of calculated results to experimental data and distribution of the relative errors: model M1 – area ratio.

3.2.1. *Models comparison*

The performances achieved by the models in this study are compared with the original results and summarized in Table 2. In particular, considering the calculation of the entrainment ratio with the working fluid R141b using the models M1, M2 and M4, the mean relative error committed by our simulations (17.53%, 6.11% and 6.95%, respectively) is slightly higher than that obtained by the original works (11.84%, 4.56% and 4%, respectively). Instead, with the models M3 and M5 the mean error is about 4.5% and 3%, respectively, in both simulations. As already remarked, the obtained numerical results are influenced by several factors, like the thermodynamic library adopted (i.e. the thermodynamics properties of the working fluid in models M1, M2 and M3) and the definition of the tolerances employed in the computational procedure. Therefore, the errors obtained are not necessary equal to those reported by the works taken as reference.

The model M1 results in higher errors if compared to the other implemented models, however this model is the only one that has results not depending on the working fluid considered (Fig. 4). The main reason of this behavior is that this model does not require the ejector geometry as an input, but is evaluated as the result of the model iterative procedure. Indeed, from Fig. 4 we may notice that the maximum error frequency for model M1 is uniformly dispersed on the five different classes. This is not true for the other models, i.e. for R245fa the error has a peak of frequency of 50% in the third and/or fourth classes. This consideration may suggest that the model M1 outputs do not depend on the working fluids itself. Indeed, despite all tested models have different mathematical structures, the main difference between the model M1 and the others is that model M1 does not require the geometrical information as input. For this reason, we may conclude that this is the reason why model M1 results show a relative independency on the working fluids.

The geometric parameter ϕ ($=A_2/A_t$) is well predicted by the model with all the considered benchmarks. Indeed, the mean relative error with R141b, R236fa and R245fa is equal to 1.75%, 4.9% and 0.55%, respectively, and the maximum error is less than 7% in all cases (Fig. 3). The model M2 is somewhat penalized by some less satisfactory results obtained with R141b; however, around the 85% of the relative errors are less than 10% (Fig. 5). The model M3 worsens its good performance with the R245fa benchmark, for which the mean relative error is equal to 17% and the maximum error exceeds the 22%

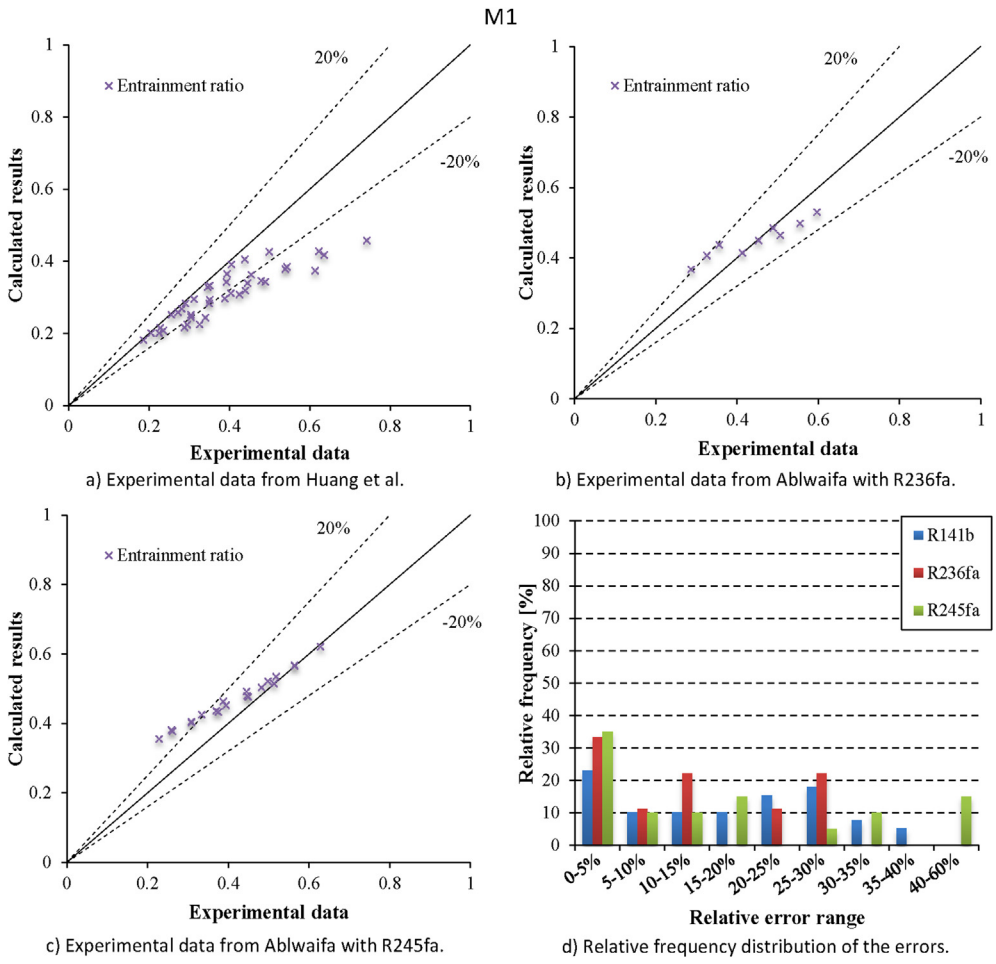

Fig. 4 – Comparison of calculated results to experimental data and distribution of the relative errors: model M1 – entrainment ratio.

(Fig. 6). The model M4, which involves the use of variable heat capacity ratio, gets quite good results but the maximum error with R141b is very high (equal to 27.5%). However, the 75% of the relative errors are less than 10% and its performance improves with R236fa (Fig. 7). Finally, the model M5 is able to keep relative errors within 17.8% with all the experimental data (Fig. 8). The best performances (in terms of prediction of the entrainment ratio) are achieved with the models M2, M3 and M5, even if the model accuracy is sensible to the working fluids. The comparison among the histograms of the models highlights that the models M3 and M5 get the best results with the R141b benchmark, while R245fa provides the worst performance with all the models, especially with M3 and M5. The nature of the working fluid is therefore very important and has a great influence on the performance prediction of the lumped parameter models which are geometry depending.

A useful parameter for the comparison is the computational effort (CE) required by the numerical simulation. It is calculated on the basis of the time spent for the calculation, in relative terms, taking as reference the model M2. The results concerning the computational effort require some comments. First, the same operating conditions, corresponding to the critical mode, have been chosen for all the models. Thus, in these conditions, the model M2 ($CE = 1$) is the fastest to run, followed by the model M4 ($CE = 1.4$) although it requires an iterative cycle for each part of the ejector. A little heavier from the computational point of view are the model M3 ($CE = 3.8$) and M5 ($CE = 9.6$). The most onerous model is M1 ($CE = 11.6$), penalized by the fact that requires a computational procedure with two iteration processes.

We may conclude that all the models compared in this section show a good prediction of the entrainment ratio. On the other hand, the model M1 shows a wider range of application because geometrical inputs are not required and an optimized geometry is provided as an output. Therefore, in the following of this study, it has been used for screening the working fluids and to study the influence of the working fluid over ejector performance. Once selected the working fluid, the other models, such as the model M5 can be used for evaluating the performance of a fixed geometry ejector in future works.

3.2.2. *Sensitivity analysis on ejector efficiencies*

A sensitivity analysis has been performed to assess the variability of the predictions due to changes in the assumed parameters. Therefore, the isentropic efficiencies and the loss coefficient have been varied of ±0.05 from the original value.

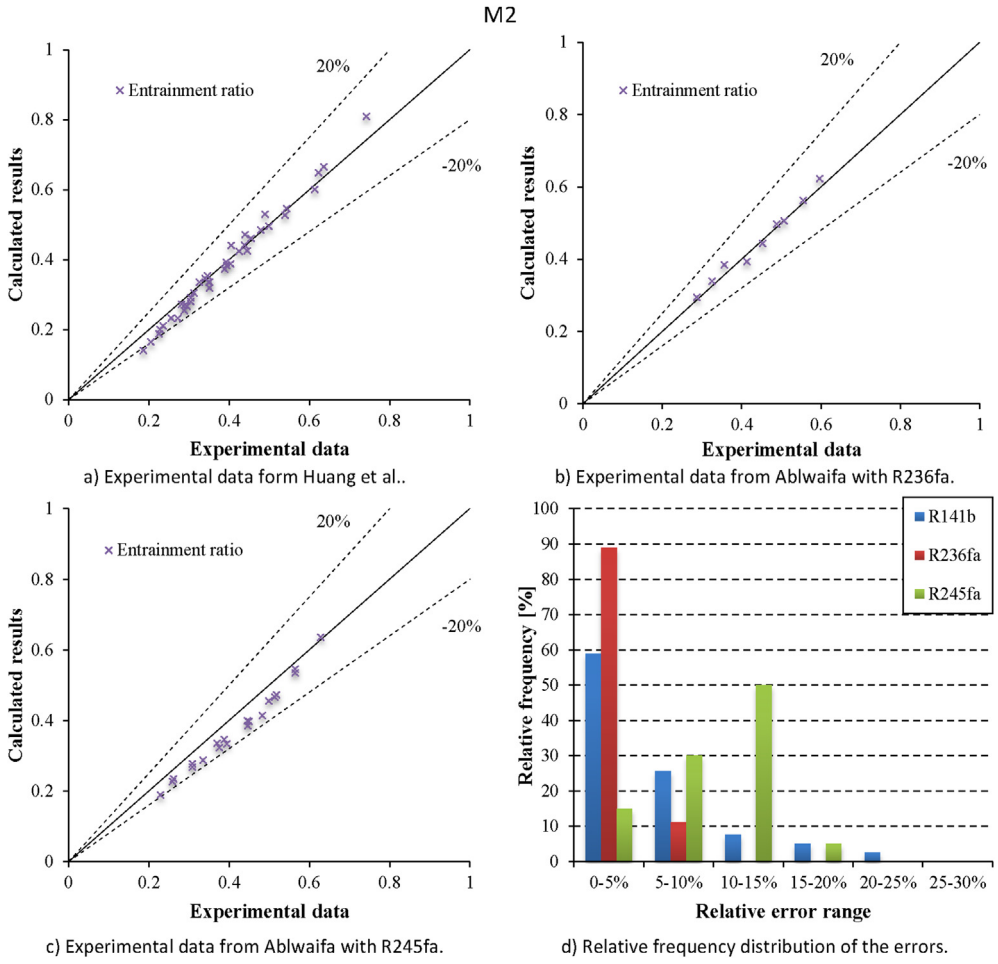

Fig. 5 – Comparison of calculated results to experimental data and distribution of the relative errors: model M2 – entrainment ratio.

The reported results (Fig. 2) refer to the absolute changes in percentage of the calculated entrainment ratio. In the model M1, the isentropic efficiencies η_n, η_m and η_d have an appreciable effect on results (−4.6 to 3.9%, −4.9 to 4.1% and −5.1 to 4.6%, respectively). Instead, the models M2, M3 and M4 have less sensitivity to the efficiency parameters and the calculated entrainment ratio always falls in the range −2.5 to 2.5%. The study shows, moreover, that the model M5 has a high sensitivity to the expansion coefficient ψ (−8.8 to 10.1%) and a moderate sensitivity to the nozzle efficiency η_n (−1.9 to 2.2%). The efficiency of the mixing chamber η_m, instead, has practically no effect on the prediction of the entrainment ratio (−0.3 to 0.3%).

4. Effect of the working fluid on the ejector performance

In this section, the effect of the working fluid on the ejector performance (ω, the entrainment ratio) and ejector refrigeration cycle (*COP*, the coefficient of performance) is studied. This section is structured as follows, at first the ejector refrigeration cycle considered is detailed, at second the simulation parameter and solution procedure is explained and at last the analysis results are outlines.

4.1. *Ejector refrigeration cycle*

A subcritical cycle operating, using a low grade energy source, has been considered for the analysis, due to the ability of the selected models to describe only subcritical ejection cycles. In fact, the analyzed models do not account for the significant changes of the isentropic coefficients and thermophysical properties that occur in the region close to the critical point. If considering transcritical and supercritical ejection cycles, the appropriate modifications of the gasdynamic relationships will be required along with substantial modifications of the discussed models. The range of operating conditions considered in the following of this paper and the cycle configuration is the one typically employed for the case of solar energy sources or water heat, such as detailed in previous papers (Abdulateef et al., 2009; Chen et al., 2014b,c; Dorantes and Lallemand, 1995; Kasperski and Gil, 2014). The system considered is shown in Fig. 9 and consists of a generator,

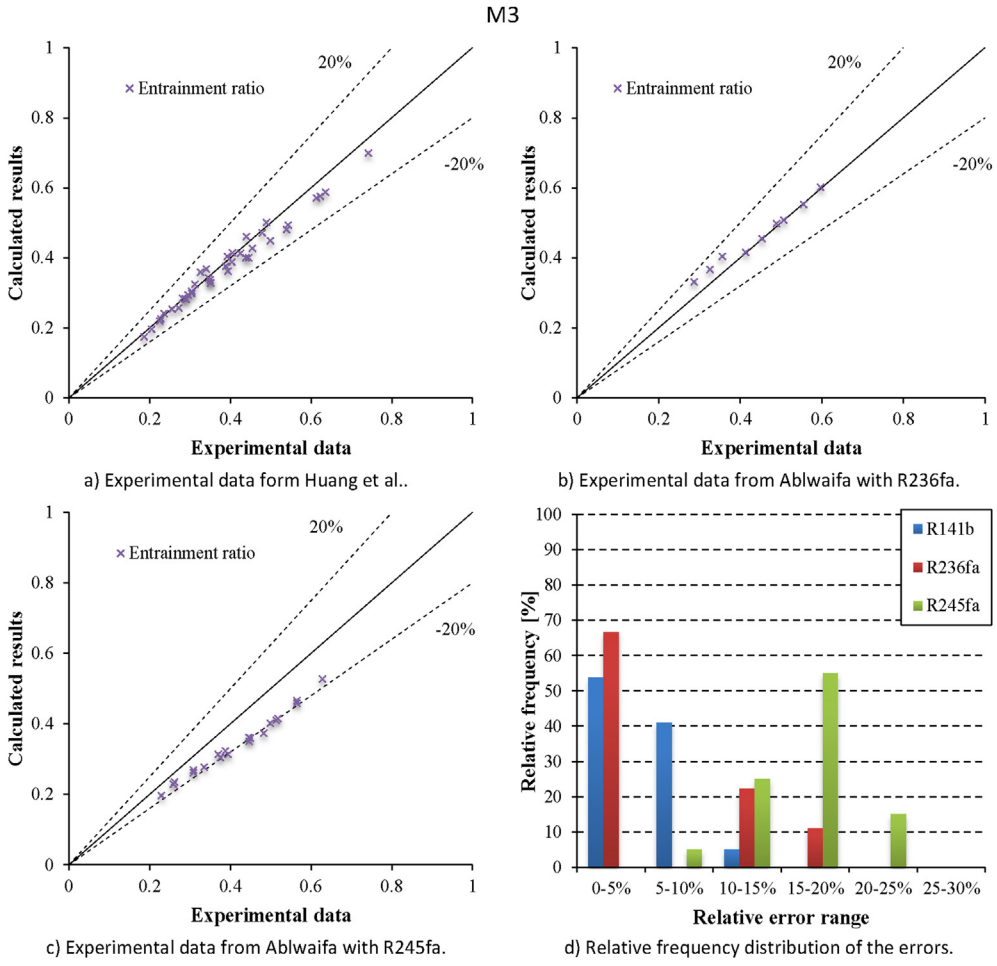

Fig. 6 – Comparison of calculated results to experimental data and distribution of the relative errors: model M3 – entrainment ratio.

a condenser, an evaporator, an ejector, a circulation pump and a throttle valve. The low-grade heat energy is delivered to the generator for the working fluid vaporization. The high-pressure vapor (the primary flow) flows out from the generator enters into ejector nozzle and draws low-pressure vapor from the evaporator (the secondary flow). The two flows mix, the pressure is raised in the ejector diffuser and the flow reaches the condenser where it changes phases from vapor to liquid rejecting heat. Once condensation takes place the flow is divided in two parts, one heading to the generator and the ejector and another to the evaporator.

4.2. *Simulation parameters and solution procedure*

Our analysis is conducted through the mathematical model M1 and the effect of generator, evaporator and condenser temperature over the entrainment ratio and the COP has been investigated for different working fluids in the typical operating conditions of waste heat and solar energy sources. At first, the influence of the generator pressure is analyzed and the operating conditions assumed are: $T_e = 10$ °C, $T_c = 40$ °C and $T_g = 70–180$ °C (if available, based on the critical temperature of the fluid). At second, the effect of the other operating conditions on the ERS performance has been evaluated. The generator temperature is assigned and equal to $T_g = 90$ °C. This value was chosen so that it was feasible by all the tested fluid. The ranges considered for the evaporator and condenser temperature are $T_e = 5–15$ °C and $T_c = 30–50$ °C.

The tested refrigerants are: propane (R290), butane (R600), iso-butane (R600a), pentane (R601), iso-pentane (R601a), R134a, R141b and R152a. The selection includes the most commonly fluids used in the past and nowadays in subcritical ejector systems (such as halocarbons R141b and R134a) and the refrigerants that could replace them in the future due to their low GWP value (such as R152a and hydrocarbons). Table 3 summarizes the properties of the working fluids analyzed. Among the tested refrigerants, the pentane R601 has a relatively high critical temperature ($T_{cr} = 196.7$ °C), which provides a wide operating temperature range above the ambient temperature.

In the paper of Chen et al. (2014a) the calculation procedure for the refrigeration cycle is reported and the present work has followed their solution method and assumptions. According with the assumptions of the model, the primary and

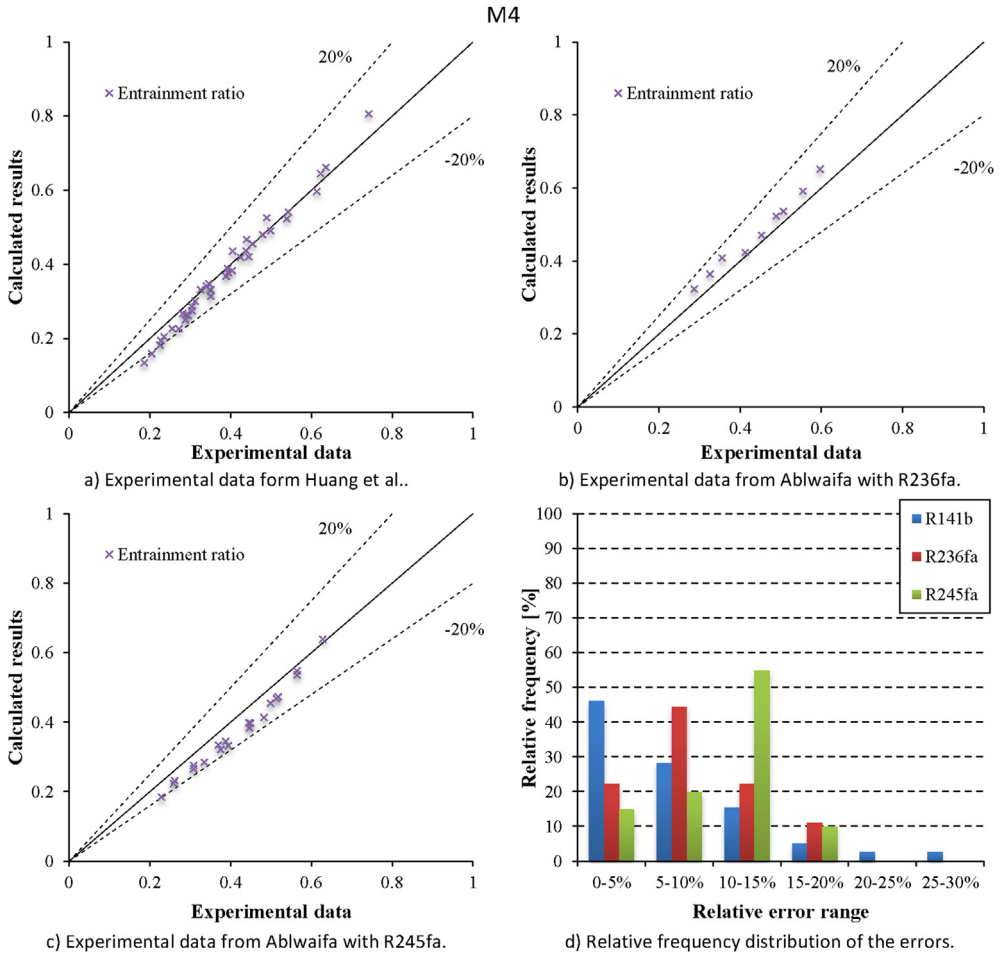

Fig. 7 – Comparison of calculated results to experimental data and distribution of the relative errors: model M4 – entrainment ratio.

secondary flow inlets are assumed as saturated vapor. In this analysis the efficiency coefficients are assumed as $\eta_n = 0.95$, $\eta_m = 0.85$ and $\eta_d = 0.9$. These values are representative of the most common efficiencies used and are in the range of variability reported in the literature (Besagni et al., 2014; Liu and Groll, 2013; Varga et al., 2009b). Moreover, the review of Liu (2014) presents a summary of the ejector efficiencies used in lumped parameter models. A sensitivity analysis over the ejector efficiency values has been performed and is presented in Section 4.3.3.

4.3. *Simulation results*

4.3.1. *Influence of generator temperature*

The numerical results are reported in Fig. 10. It should be noted that the effects described in this discussion refer to optimum performance evaluation with a corresponding suitable ejector area ratio ϕ (A_2/A_t), which are different from a fixed-geometry ejector working under different conditions. As expected in these conditions, the entrainment ratio ω and the *COP* generally increase with a rise in T_g for all working fluids. In fact, the pressure and enthalpy of the primary flow increase with the T_g, and a higher T_g causes a better entrainment effect at a given T_c and T_e. More secondary flow could therefore be entrained into the ejector, resulting in a higher ω. This is obtained through an adjustment of the area ratio to provide sufficient flow area for the flow. The trend of the area ratio as a function of T_g is shown in Fig. 11 resulting coherent with the literature (Chen et al., 2014c; Yen et al., 2013). Indeed, the area ratio grows with T_g as a result of the increase of the entrainment effect. However, the working fluid affects this trend and the area ratio adjustment is different according to the nature of the refrigerant and to the operating condition field in which the ejector works. The average changes of the area ratio ϕ are reported in Table 4. They express the mean variation of ϕ, calculated from 1 °C change in each temperature, in the considered temperature range. The average increases of ϕ are in the range 9.37–38.58% depending on the working fluid: the hydrocarbons R601 and R601a have the greatest average increase of ϕ (equal to 38.58% and 30.30%, respectively), probably due to the higher values of T_g. The R290 has, instead, the lowest average increase of ϕ: 1 °C increase in T_g improves ϕ by approximately 9.37%. In the same operating conditions range, R141b has an average increase equal to about 19%. Therefore, for a variable-geometry ejector, the ejector area ratio grows

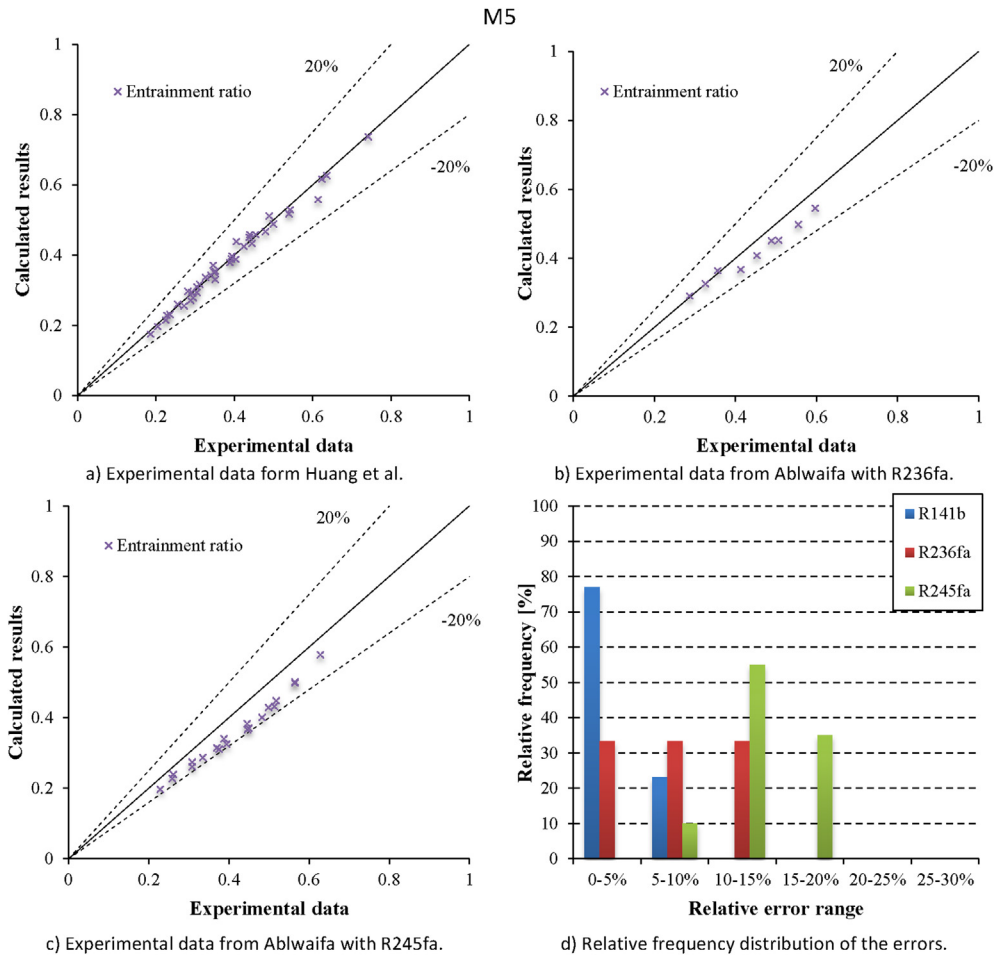

Fig. 8 – Comparison of calculated results to experimental data and distribution of the relative errors: model M5 – entrainment ratio.

with T_g to allow the entrance of more secondary fluid, which involves the rise of ω and COP.

The COP trend with which varies as a function of T_g is generally similar to that of ω, because COP and ω are directly related with one another for all the working fluid used.

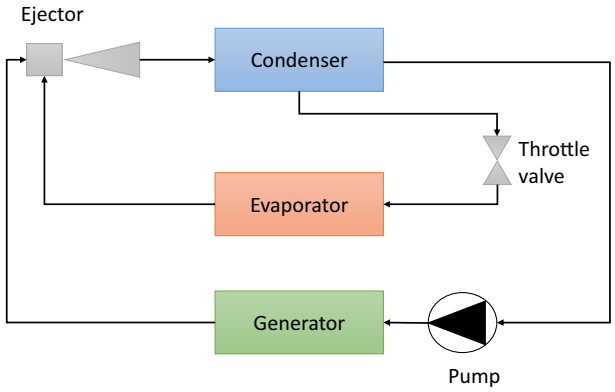

Fig. 9 – Ejector refrigeration system.

However, the reader should consider that the relation between COP and ω is also dependent on fluid. Indeed, for a given entrainment ratio, the COP still depends on enthalpies of the employed refrigerant. For a fixed-geometry ejector, instead, each ejector with a specific area ratio ϕ has its own optimum T_g, at where the maximum COP could be obtained (Selvaraju and Mani, 2006). It is possible to observe that the calculated COP from the model increase nearly linearly with increasing of T_g, as reported in literature (Yapıcı et al., 2008). The average changes in performance are reported in Table 4.

The dry fluids generally perform better with higher values of ω than the wet fluids. In addition, R600 and R600a have wider ranges of T_g thanks to their higher critical temperatures compared to the rest candidates. However, the analysis shows that the halocarbon refrigerant R134a is the best choice for ERS that work at low generator temperature (T_g = 70–100 °C), both in terms of entrainment ratio (ω = 0.16–0.35) and coefficient of performance (COP = 0.13–0.27). With regard to the COP, the more environmentally friendly refrigerant R152a can be a good solution for medium temperatures (T_g = 90–100 °C). Moreover, R152a has a greater average increase of COP than R134a: 1 °C change of T_g grows the COP by around 0.61%, as

Table 3 – Environmental, safety and thermophysical properties of the working fluid considered.

Refrigerant	R134a	R141b	R152a	R290	R600	R600a	R601	R601a
GWP (100 yr)	1370	717	133	20	20	20	20	20
ODP	0	0.12	0	0	0	0	0	0
Safety group	A1	A2	A2	A3	A3	A3	A3	A3
Wet/dry	Wet	Dry	Wet	Wet	Dry	Dry	Dry	Dry
Molecular mass	102.0	116.9	66.1	44.1	58.1	58.1	72.15	72.15
Boiling point [°C]	−26.1	32.1	−24.0	−42.1	−0.5	−11.8	36.1	27.8
Latent heat at 10 °C [kJ kg^{-1}]	190.9	233.1	295.8	360.3	376.1	344.6	377.6	356.5
Critical temperature [°C]	101.1	204.4	113.3	96.7	152.0	134.7	196.6	187.2
Critical pressure [kPa]	4059	4212	4520	4247	3796	3629	3370	3378

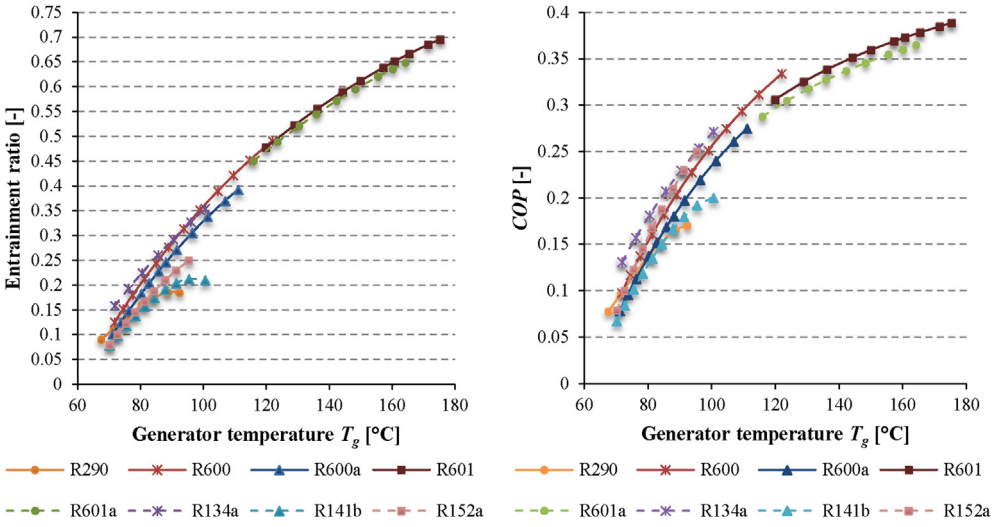

Fig. 10 – Entrainment ratio and COP as function of the generator temperature (T_e = 10 °C, T_c = 40 °C).

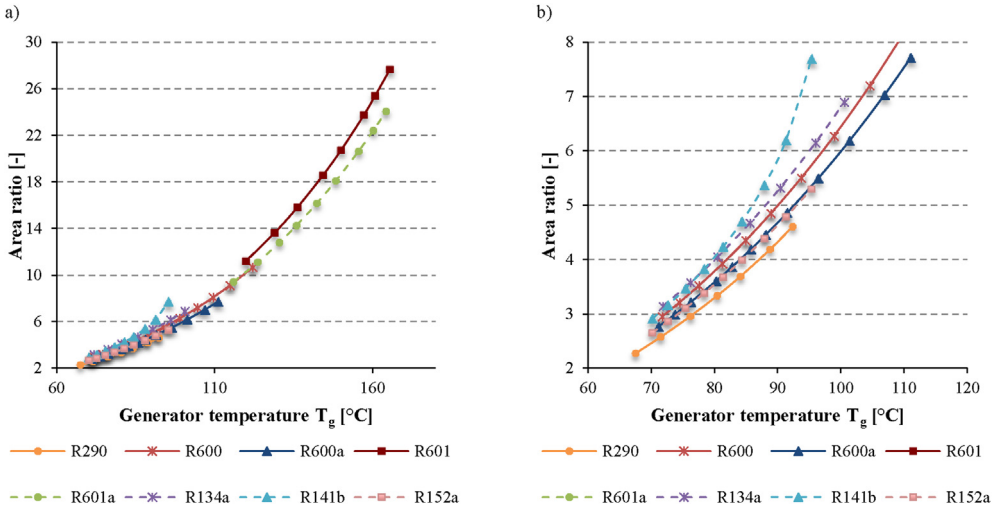

Fig. 11 – Area ratio as function of the generator temperature (T_e = 10 °C, T_c = 40 °C) – a) in the entire range of generator temperature; b) in a restricted range of generator temperature.

shown in Table 4. Considering that R134a and R152a are labeled in A1 and A2 safety groups (Table 3), respectively, they are risk-free from the toxicity and flammability point of view. However, due to the EU Regulation 517/2014, R134a must be replaced because of their high GWP values.

The halocarbon compounds tested have a limited range of operating conditions due to the low critical temperature.

Table 4 – Average changes in performance and area ratio in function of the generator, evaporator and condenser temperatures calculated from 1 °C change in each temperature.

	Refrigerant	R134a	R141b	R152a	R290	R600	R600a	R601	R601a
T_g	$\Delta\omega$ [%]	0.682	0.433	0.679	0.381	0.727	0.730	0.149	0.159
	ΔCOP [%]	0.489	0.437	0.614	0.372	0.469	0.492	0.392	0.409
	$\Delta\phi$ [%]	13.07	18.95	10.49	9.37	15.30	12.38	38.58	30.30
T_e	$\Delta\omega$ [%]	1.512	0.660	1.104	0.396	1.214	0.993	1.492	1.512
	ΔCOP [%]	1.273	0.629	1.050	0.397	0.991	0.819	1.167	1.176
	$\Delta\phi$ [%]	3.73	2.09	2.81	1.16	4.22	3.24	3.98	3.70
T_c	$\Delta\omega$ [%]	−1.764	−1.413	−1.762	−1.759	−2.042	−1.833	−2.074	−2.045
	ΔCOP [%]	−1.392	−1.223	−1.570	−1.606	−1.514	−1.360	−1.492	−1.459
	$\Delta\phi$ [%]	−24.25	−16.94	−18.84	−16.56	−22.46	−19.39	−26.70	−23.97

Thus, in order to work in a higher range of generator temperature, the hydrocarbons represent a valid alternative. In particular, R600a can replace R134a in European refrigerators with slight modifications of refrigeration and air conditioning systems (Mota-Babiloni et al., 2015). The graphs show that each hydrocarbon has its own operating range related to the molecular mass of the compound, as pointed out in Kasperski and Gil (2014) too. In fact, the generator temperature range increase with the hydrocarbon molar mass, from the propane (R290) to the pentane (R601). In particular, the working fluid R290, able to work with $T_g = 70–95$ °C, loses the competition in terms of performance with the halocarbon compounds, but the heavier hydrocarbons achieve better performance at high generator temperature ($T_g = 100–180$ °C). For the R290 and the R141b, a maximum value of ω is observed. In these operating conditions, the best working fluids are R600 at medium temperatures ($T_g = 100–130$ °C) with $COP = 0.23–0.34$ and R601 at high generator temperatures ($T_g = 130–180$ °C) with $COP = 0.30–0.39$. Therefore, R600 and R601 are promising candidates for the ejector refrigeration system. One Celsius degree increase in T_g improves ω and COP of R600 by approximately 0.73% and 0.47%, respectively. For R601 ω and COP improvements are around 0.15% and 0.39%, respectively. However, they are classified in A3 safety group and thus their flammability is to be taken into account in ejector applications.

The entrainment ratio, COP and area ratio ranges for all the working fluids considered are summarized in Table 5. It also

Table 5 – Entrainment ratio, COP and area ratio ranges as function of operating conditions according to the working fluids considered and comparison between the current study and (Chen et al., 2014c).

		a) Generator temperature T_g			b) Evaporator temperature T_e			c) Condenser temperature T_c		
		ω [–]	COP [–]	ϕ [–]	ω [–]	COP [–]	ϕ [–]	ω [–]	COP [–]	ϕ [–]
R134a	(Chen et al., 2014c)	$T_g = 80–103$ °C			$T_e = 0–16$ °C			$T_c = 27–43$ °C		
		0.21–0.41	0.18–0.34	3.87–6.80	0.21–0.50	0.12–0.41	5.18–6.12	0.15–0.71	0.12–0.61	4.01–8.66
	Current study	$T_g = 72–100$ °C			$T_e = 8–15$ °C			$T_c = 30–47.5$ °C		
		0.16–0.35	0.13–0.27	3.14–6.89	0.24–0.35	0.19–0.27	5.20–5.46	0.11–0.42	0.08–0.33	3.71–7.95
R141b	Current study	$T_g = 70–100$ °C			$T_e = 5–15$ °C			$T_c = 30–50$ °C		
		0.08–0.21	0.07–0.20	2.91–7.69	0.14–0.21	0.12–0.18	4.23–4.44	0.04–0.32	0.03–0.28	2.98–6.37
R152a	(Chen et al., 2014c)	$T_g = 90–113$ °C			$T_e = 0–16$ °C			$T_c = 27–43$ °C		
		0.26–0.47	0.22–0.39	3.97–6.88	0.17–0.43	0.10–0.35	4.05–4.75	0.11–0.67	0.10–0.57	3.13–6.80
	Current study	$T_g = 70–95$ °C			$T_e = 5–15$ °C			$T_c = 30–50$ °C		
		0.08–0.25	0.07–0.22	2.65–5.29	0.22–0.33	0.19–0.29	4.50–4.78	0.08–0.43	0.07–0.39	3.14–6.91
R290	(Chen et al., 2014c)	$T_g = 80–104$ °C			$T_e = 0–16$ °C			$T_c = 27–43$ °C		
		0.14–0.31	0.14–0.31	3.30–5.65	0.18–0.44	0.10–0.36	4.34–5.02	0.11–0.68	0.10–0.58	3.42–6.97
	Current study	$T_g = 67–92$ °C			$T_e = 5–15$ °C			$T_c = 30–42.5$ °C		
		0.09–0.18	0.08–0.17	2.27–4.60	0.10–0.14	0.09–0.13	3.79–3.90	0.08–0.30	0.08–0.28	3.53–5.60
R600	(Chen et al., 2014c)	$T_g = 75–130$ °C			$T_e = 0–16$ °C			$T_c = 27–43$ °C		
		0.30–0.78	0.24–0.53	4.29–16.7	0.30–0.71	0.18–0.53	6.56–8.26	0.27–0.93	0.20–0.70	5.21–11.7
	Current study	$T_g = 72–122$ °C			$T_e = 5–15$ °C			$T_c = 30–47.5$ °C		
		0.13–0.49	0.10–0.33	2.95–10.7	0.23–0.35	0.16–0.26	4.79–5.21	0.11–0.46	0.07–0.34	3.55–7.48
R600a	(Chen et al., 2014c)	$T_g = 75–130$ °C			$T_e = 0–16$ °C			$T_c = 27–43$ °C		
		0.26–0.68	0.21–0.50	3.88–14.6	0.29–0.66	0.17–0.49	6.07–7.41	0.25–0.88	0.18–0.66	4.79–10.4
	Current study	$T_g = 72–111$ °C			$T_e = 5–15$ °C			$T_c = 30–47.5$ °C		
		0.10–0.39	0.08–0.27	2.76–7.61	0.21–0.31	0.15–0.23	4.47–4.79	0.10–0.42	0.07–0.31	3.40–6.79
R601	Current study	$T_g = 120–175$ °C			$T_e = 7–15$ °C			$T_c = 30–45$ °C		
		0.47–0.70	0.31–0.39	11.2–32.6	0.23–0.35	0.16–0.26	5.28–5.60	0.15–0.46	0.10–0.32	4.17–8.18
R601a	Current study	$T_g = 116–164$ °C			$T_e = 7–15$ °C			$T_c = 30–45$ °C		
		0.45–0.65	0.29–0.36	9.41–24.0	0.25–0.38	0.17–0.27	4.95–5.24	0.17–0.47	0.11–0.33	3.95–7.55

Operating conditions of Chen et al. (2014c): a) $T_e = 10$ °C, $T_c = 35$ °C; b) $T_g = 95$ °C, $T_c = 35$ °C; c) $T_g = 95$ °C, $T_e = 10$ °C.
Ejector efficiencies: $\eta_n = \eta_m = \eta_d = 0.9$.

reported the results carried out by Chen et al. (2014c) for some refrigerants examined. Even if the two works have not considered the same operating conditions and ejector efficiencies, the numerical results are qualitatively very similar. However, the values obtained by Chen et al. (2014c) are slightly higher mainly because of the lower condenser temperature and the higher generator temperature assumed, as well as a greater value of the mixing efficiency.

In this range of generator temperature, the heat source for the vapor production could be provided by waste heat and solar energy. Considering a solar drive, several types of collectors can be employed according to the generator temperature. The flat-plate solar collectors are suitable up to temperature less than 100 °C. For the medium temperature range 100–150 °C, the employment of the evacuated tube solar collectors is recommended. The high temperature, greater than 150 °C, requires concentrating solar collectors, such as parabolic-trough. According to the considered temperature demand, the ejector systems can be mainly used in air conditioning applications (motor vehicle, office, building), but also in domestic, commercial and industrial (chemical, pharmaceutical,...) fields for refrigeration purpose (Sarbu and Sebarchievici, 2013). However, the operating conditions and the working fluid selection for a specific application is affected by several factors, such as the economic feasibility (in order to justify the temperature level), the heat source availability, the environment (that influence the condition to which release heat) and the evaporator conditions (that determine the cooling effect and thus the potential application).

4.3.2. *Influence of evaporator and condenser temperature*

The results are shown in Fig. 12 and summarized in Table 5. According to the results, an increase in T_e leads to a rise in the entrainment ratio ω and *COP*. However, the condenser temperature has more influence than the evaporator temperatures on the ejector performance. In fact, the average increases of ω and *COP* are 1.41–2.05% and 1.22–1.61% (in absolute value), while for T_e change are equal to 0.40–1.51% and 0.40–1.27%, respectively. For a fixed-geometry ejector, it

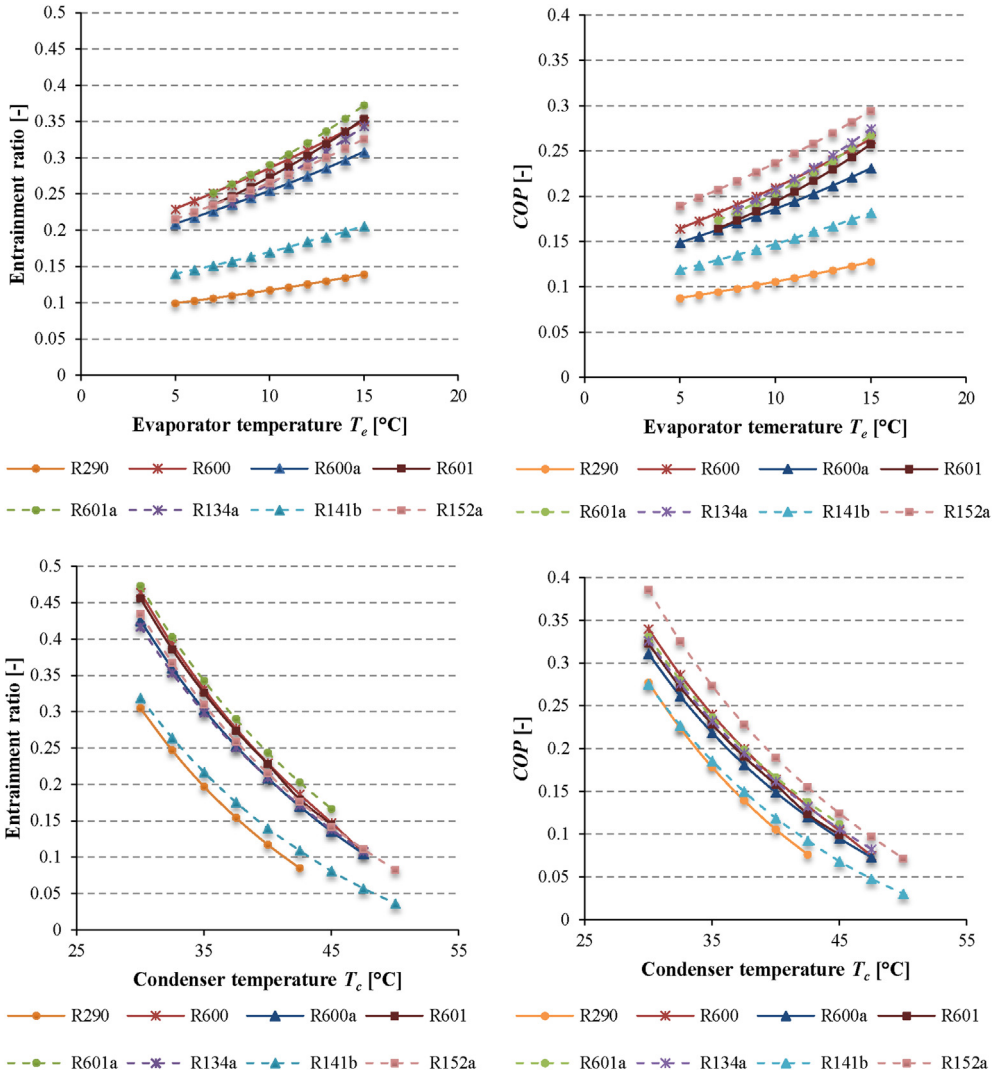

Fig. 12 – Entrainment ratio and COP as function of the evaporator temperature (T_g = 90 °C, T_c = 40 °C) and condenser temperature (T_g = 90 °C, T_e = 10 °C).

is known that there exists a critical condenser pressure p_c^*: the entrainment ratio is independent of the condenser temperature T_c when p_c is lower than the critical value; a slightly further increase of p_c beyond p_c^* will cause ω to drop sharply (Huang et al., 1999). With a variable-geometry ejector, instead, an increase in T_c leads to a gradual decrease in ω and *COP*. This is because less secondary flow can be entrained into the ejector if the backpressure increases. Another reason might be that an increase in the p_c will force the shock to pass through the mixing section and move towards the nozzle exit, which limits the entrainment effect (Sun, 1996).

As a result, a high T_e and a low T_c will always be good for the ejector operation and the whole system performance. However, the evaporator and the condenser temperature should be chosen according to the desirable and feasible cooling effect and on the basis of the environmental conditions, respectively. The generator temperature has a lower effect on the average changes of ω (0.15–0.73%) and *COP* (0.37–0.49%), but generally it is possible to exploit a wider range of temperature variation compared with the evaporator and condenser temperature. In these operating conditions, the R601a achieves the maximum entrainment ratio, varying both the evaporator temperature ($\omega = 0.25$–0.37) and the condenser temperature ($\omega = 0.17$–0.47). In both cases, the maximum *COP* is instead obtained by R152a (*COP* = 0.19–0.30 and *COP* = 0.07–0.39, respectively).

Fig. 13 shows the area ratio as a function of T_e and T_c. As with ω and *COP*, the evaporator temperature less affects the area ratio values then the condenser temperature: 1 °C increase in T_e and T_c adjusts ϕ by 1.16–4.22% and 16.56–26.70% (in absolute value), respectively. The average changes of ϕ for each working fluid are summarized in Table 4.

4.3.3. *Sensitivity analysis*

The sensitivity analysis has been performed in order to determine the influence of the isentropic efficiency coefficients (η_n, η_m and η_d) on the numerical results. For this evaluation, the ejector component efficiencies values have been varied of ±0.025 from the original values. The study shows that the model has a quite high sensitivity to the isentropic efficiencies, especially to the diffuser efficiency η_d, both for ω and *COP*. In fact, varying the isentropic coefficient by only ±2.5 percentage points, the predicted value of the entrainment ratio undergoes a variation in the range of −4.90 to 4.29% while those of the *COP* is equal to −3.78 to 3.31%. The efficiency of the mixing chamber η_m and of the nozzle η_n have a slightly lower effect on the prediction of the entrainment ratio (−3.72 to 3.62% and −3.47 to 3.12%, respectively) and of the *COP* (−2.83 to 2.77% and −2.72 to 2.49%, respectively).

5. Conclusions

This paper studies the effect of generator, evaporator and condenser temperature over the ejector performance for different working fluids by using lumped parameter models. The working fluid studies and the range of operating conditions are typical of waste heat and solar energy sources.

In the first part, five thermodynamic models have been selected, implemented and validated with several benchmarks from the literature. The experimental data have been selected from different studies for considering different working conditions, working fluid and geometries. With the tested models, quite good results have been achieved: the mean values of the relative errors of the models are about between 3% and 17%.

In the second part, the model M1 is selected in order to carry out a numerical analysis, testing several working fluids (both dry and wet) at different operating conditions. This model has been selected because its results are quite independent on the working fluid and it does not require geometrical parameters in input. It was found that, regardless of the working fluid, the entrainment ratio and the *COP* increase with increasing of generator temperature and evaporator temperature, while an increasing condenser temperature leads a decrease in the ejector performance. For this occurrence, the ejector area ratio needs to be adjusted to maintain optimum performance of an ERS under different

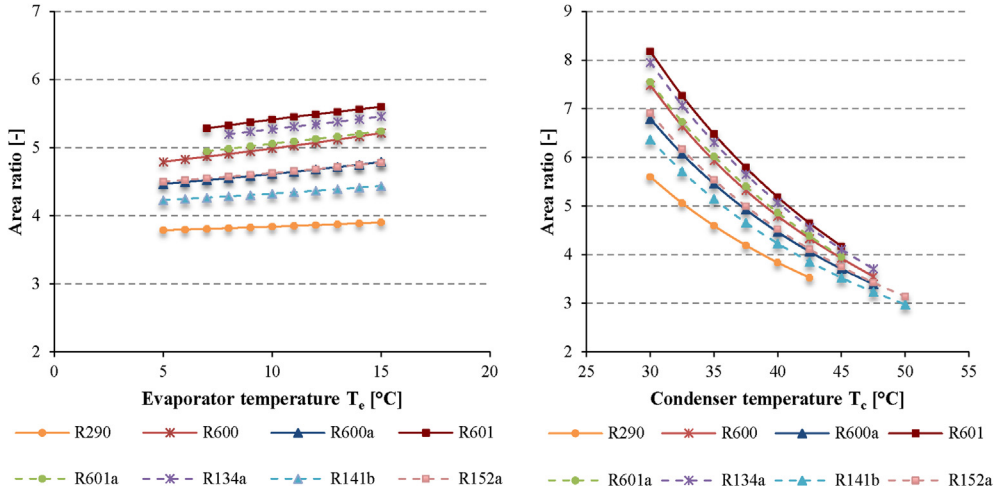

Fig. 13 – Area ratio as function of the evaporator temperature ($T_g = 90$ °C, $T_c = 40$ °C) and condenser temperature ($T_g = 90$ °C, $T_e = 10$ °C).

working conditions and the degree of adaptation depends on refrigerant. The variable-geometry ejectors can play an important role in achieving optimum performance and widen the operating conditions. Indeed, a variable-geometry ejector seems a very promising solution to ensure that the ERS operates at its optimum conditions. For each fluid is then found an application field according to the performance reached in specific ranges of operating conditions. The hydrocarbon compounds R600 and R601 are good solutions for the ERS that operated at high generator temperature (T_g = 100–150 °C), reaching COP = 0.3–0.4. While, for T_g less than 100 °C, the halocarbon compounds R134a and R152a achieved the best performance (COP = 0.15–0.25). Finally, it was observed that the ejector efficiencies are crucial parameters in the LPM model. Indeed, the sensitivity analysis has shown that the model has high sensitivity to the efficiencies, leading remarkable variations for the entrainment ratio and COP. The loss coefficients are supposed constant but it is known from literature that they depend upon the working fluid, the operating conditions, the geometry and the local phenomena. Thus, the performance prediction of the LPM can be improved using variable efficiencies as suggested by He et al. (2009). The variable ejector efficiencies can be obtained by using a Computational Fluid Dynamic approach (Besagni et al., 2014), an experimental investigation (Liu and Groll, 2013) or data from the literature (Chen et al., 2014b). Future studies should take into account and evaluate the role of variable efficiencies while evaluating the role of working fluids over ejector performance.

Acknowledgment

The authors would like to thank the anonymous reviewers for their valuable comments and suggestions to improve the quality of the paper.

REFERENCES

Abdulateef, J.M., Sopian, K., Alghoul, M.A., Sulaiman, M.Y., 2009. Review on solar-driven ejector refrigeration technologies. Renew. Sustain. Energy Rev. 13, 1338–1349.

Ablwaifa, A.E., 2006. A Theoretical and Experimental Investigation of Jet-Pump Refrigeration System. University of Nottingham.

Alexis, G.K., Katsanis, J.S., 2004. Performance characteristics of a methanol ejector refrigeration unit. Energy Convers. Manag. 45, 2729–2744.

Angelino, G., Invernizzi, C., 2008. Thermodynamic optimization of ejector actuated refrigerating cycles. Int. J. Refrigeration 31, 453–463.

Aphornratana, S., Chungpaibulpatana, S., Srikhirin, P., 2001. Experimental investigation of an ejector refrigerator: effect of mixing chamber geometry on system performance. Int. J. Energy Res 25, 397–411.

ASHRAE, 2010. Designation and Safety Classification of Refrigerants.

Banasiak, K., Palacz, M., Hafner, A., Buliński, Z., Smołka, J., Nowak, A.J., Fic, A., 2014. A CFD-based investigation of the energy performance of two-phase R744 ejectors to recover the expansion work in refrigeration systems: an irreversibility analysis. Int. J. Refrigeration 40, 328–337.

Bell, I.H., Wronski, J., Quoilin, S., Lemort, V., 2014. Pure and pseudo-pure fluid thermophysical property evaluation and the open-source thermophysical property library CoolProp. Ind. Eng. Chem. Res. 53, 2498–2508.

Ben Mansour, R., Ouzzane, M., Aidoun, Z., 2014. Numerical evaluation of ejector-assisted mechanical compression systems for refrigeration applications. Int. J. Refrigeration 43, 36–49.

Besagni, G., Mereu, R., Colombo, E., 2014. CFD study of ejector efficiencies. In: ASME 2014 12th Biennial Conference on Engineering Systems Design and Analysis. ESDA2014–20053, Copenhagen, Denmark, June 25–27, 2014. V02T11A004.

Bolaji, B.O., Huan, Z., 2013. Ozone depletion and global warming: case for the use of natural refrigerant – a review. Renew. Sustain. Energy Rev. 18, 49–54.

Cardemil, J.M., Colle, S., 2012. A general model for evaluation of vapor ejectors performance for application in refrigeration. Energy Convers. Manag. 64, 79–86.

Chen, J., Havtun, H., Palm, B., 2014a. Investigation of ejectors in refrigeration system: optimum performance evaluation and ejector area ratios perspectives. Appl. Therm. Eng. 64, 182–191.

Chen, J., Havtun, H., Palm, B., 2014b. Parametric analysis of ejector working characteristics in the refrigeration system. Appl. Therm. Eng. 69, 130–142.

Chen, J., Havtun, H., Palm, B.r, 2014c. Screening of working fluids for the ejector refrigeration system. Int. J. Refrigeration 47, 1–14.

Chen, W., Liu, M., Chong, D., Yan, J., Little, A.B., Bartosiewicz, Y., 2013a. A 1D model to predict ejector performance at critical and sub-critical operational regimes. Int. J. Refrigeration 36, 1750–1761.

Chen, X., Omer, S., Worall, M., Riffat, S., 2013b. Recent developments in ejector refrigeration technologies. Renew. Sustain. Energy Rev. 19, 629–651.

del Valle, J.G., Jabardo, J.M.S., Ruiz, F.C., Alonso, J.F.S.J., 2014. An experimental investigation of a R-134a ejector refrigeration system. Int. J. Refrigeration 46, 105–113.

Dorantes, R., Lallemand, A., 1995. Prediction of performance of a jet cooling system operating with pure refrigerants or non-azeotropic mixtures. Int. J. Refrigeration 18, 21–30.

Godefroy, J., Boukhanouf, R., Riffat, S., 2007. Design, testing and mathematical modelling of a small-scale CHP and cooling system (small CHP-ejector trigeneration). Appl. Therm. Eng. 27, 68–77.

He, S., Li, Y., Wang, R.Z., 2009. Progress of mathematical modeling on ejectors. Renew. Sustain. Energy Rev. 13, 1760–1780.

Hemidi, A., Henry, F., Leclaire, S., Seynhaeve, J.M., Bartosiewicz, Y., 2009. CFD analysis of a supersonic air ejector. Part I: experimental validation of single-phase and two-phase operation. Appl. Therm. Eng. 29 (14–15), 2990–2998.

Huang, B.J., Chang, J.M., Wang, C.P., Petrenko, V.A., 1999. A 1-D analysis of ejector performance. Int. J. Refrigeration 22, 354–364.

Kasperski, J., Gil, B., 2014. Performance estimation of ejector cycles using heavier hydrocarbon refrigerants. Appl. Therm. Eng. 71, 197–203.

Kumar, N.S., Ooi, K.T., 2014. One dimensional model of an ejector with special attention to Fanno flow within the mixing chamber. Appl. Therm. Eng. 65, 226–235.

Little, A.B., Garimella, S., 2011. Comparative assessment of alternative cycles for waste heat recovery and upgrade. Energy 36, 4492–4504.

Liu, F., 2014. Review on ejector efficiencies in various ejector systems. In: International Refrigeration and Air Conditioning Conference, Purdue.

Liu, F., Groll, E.A., 2013. Study of ejector efficiencies in refrigeration cycles. Appl. Therm. Eng. 52, 360–370.
Lucas, C., Koehler, J., 2012. Experimental investigation of the COP improvement of a refrigeration cycle by use of an ejector. Int. J. Refrigeration 35, 1595–1603.
Mota-Babiloni, A., Navarro-Esbrí, J., Barragán-Cervera, Á., Molés, F., Peris, B., 2015. Analysis based on EU Regulation No 517/2014 of new HFC/HFO mixtures as alternatives of high GWP refrigerants in refrigeration and HVAC systems. Int. J. Refrigeration 52, 21–31.
Sankarlal, T., Mani, A., 2007. Experimental investigations on ejector refrigeration system with ammonia. Renew. Energy 32, 1403–1413.
Sarbu, I., 2014. A review on substitution strategy of non-ecological refrigerants from vapour compression-based refrigeration, air-conditioning and heat pump systems. Int. J. Refrigeration 46, 123–141.
Sarbu, I., Sebarchievici, C., 2013. Review of solar refrigeration and cooling systems. Energy Build. 67, 286–297.
Sarkar, J., 2012. Ejector enhanced vapor compression refrigeration and heat pump systems—a review. Renew. Sustain. Energy Rev. 16, 6647–6659.
Selvaraju, A., Mani, A., 2006. Experimental investigation on R134a vapour ejector refrigeration system. Int. J. Refrigeration 29, 1160–1166.
Sun, D.-W., 1996. Variable geometry ejectors and their applications in ejector refrigeration systems. Energy 21, 919–929.
Varga, S., Oliveira, A.C., Diaconu, B., 2009a. Influence of geometrical factors on steam ejector performance – a numerical assessment. Int. J. Refrigeration 32, 1694–1701.
Varga, S., Oliveira, A.C., Diaconu, B., 2009b. Numerical assessment of steam ejector efficiencies using CFD. Int. J. Refrigeration 32, 1203–1211.
Vidal, H., Colle, S., 2010. Simulation and economic optimization of a solar assisted combined ejector–vapor compression cycle for cooling applications. Appl. Therm. Eng. 30, 478–486.
Yapıcı, R., Ersoy, H.K., Aktoprakoğlu, A., Halkacı, H.S., Yiğit, O., 2008. Experimental determination of the optimum performance of ejector refrigeration system depending on ejector area ratio. Int. J. Refrigeration 31, 1183–1189.
Yen, R.H., Huang, B.J., Chen, C.Y., Shiu, T.Y., Cheng, C.W., Chen, S.S., Shestopalov, K., 2013. Performance optimization for a variable throat ejector in a solar refrigeration system. Int. J. Refrigeration 36, 1512–1520.
Zhu, Y., Cai, W., Wen, C., Li, Y., 2007. Shock circle model for ejector performance evaluation. Energy Convers. Manag. 48, 2533–2541.